Received 8 May 2019; revised 10 July 2019; accepted 26 August 2019. Date of publication 6 September 2019; date of current version 30 September 2019.
The review of this article was arranged by Editor A. Nathan.

Digital Object Identifier 10.1109/JEDS.2019.2939912

A Capacitive Information-Based Force-Voltage Responsivity Stabilization Method for Piezoelectric Touch Panels

ANBIAO HUANG[1,2], SHUO GAO [1,2], YANNING DAI[1,2], VASILEIOS KITSOS[3], WENBIN TIAN [1,2], AND LIJUN XU [1,2] (Senior Member, IEEE)

1 School of Instrumentation Science and Optoelectronic Engineering, Beihang University, Beijing 100191, China
2 Beijing Advanced Innovation Center for Big Data-Based Precision Medicine, Interdisciplinary Innovation Institute of Medicine and Engineering, Beihang University, Beijing 100191, China
3 Electronic and Electrical Engineering Department, University College London, London WC1E 7JE, U.K.

CORRESPONDING AUTHOR: S. GAO (e-mail: gaooshuoo@hotmail.com)

This work was supported in part by the National Natural Science Foundation under Grant 61803017 and Grant 61827802, and in part by the Beihang University under Grant KG12090401 and Grant ZG216S19C8.

ABSTRACT Piezoelectric force touch panels receive increased attentions in recent years. However, user-induced nonstable force-voltage responsivity limits their successful use in interactive displays. In this work, touch-induced capacitive information is used for estimating contact area and touch angle, which are further employed to interpret user performed force amplitude. A promising result of improving the stability of force-voltage responsivity by 85% is achieved, enhancing user experience and advancing the development of piezoelectric force sensing in interactive displays.

INDEX TERMS Interactive display, piezoelectric material, force sensing and capacitive touch sensing.

I. INTRODUCTION

Force touch sensing has been integrated in many interactive displays of smartphones since 2015 [1], and become an important function for advanced human-machine interactivities (HMIs). Broadly implemented techniques for force sensing in interactive displays are capacitive [1], piezoresistive [2] or piezoelectric [3], [4] based. The capacitive based technique is the first generation of force sensing in commercialized smartphones and it still dominates the market. This technique utilizes the capacitance change of an additional inserted capacitive sensing layer underneath the backlight of the display. The first piezoresistive based force touch panel product released in 2018 [5], providing higher force detection resolution compared to the capacitive techniques. However, both of them increase panel's thickness, energy consumption and circuitry complexity [1]. Therefore, piezoelectric force sensing triggers researchers' interests due to its nature in passively detecting dynamic force events with high sensitivity and resolution. Furthermore, due to the dielectric property of piezoelectric materials, capacitive sensing can also be realized by piezoelectric devices [3], obtaining multidimensional sensing.

Many different piezoelectric force touch panels have been proposed [3]–[9], nevertheless, the successful use in commercialized smartphones has not been reported yet. A key factor resulting in this phenomenon is the instable force-voltage responsivity of the piezoelectric materials, indicating that the same force amplitude gives rise to different electric signals [10]. This is due to the characteristic instability of piezoelectric materials and users' touch behavior [10]. When the same force amplitude is applied by different users, the force-induced stress in z direction is not equal, due to their different touch area and orientation, resulting in poor detection accuracy.

This paper addresses the issue above with the use of the capacitive information, which is conventionally interpreted for determination of touch location and gesture sensing [11], [12], to remove the instable responsivity problem by estimating the contact area and touch direction. Experimental work presented here shows that the stability of force-voltage responsivity can be improved by 85%, compared to the study in [10].

This paper is structured as follows. Section II reviews the issue of instable force-voltage responsivity. Section III

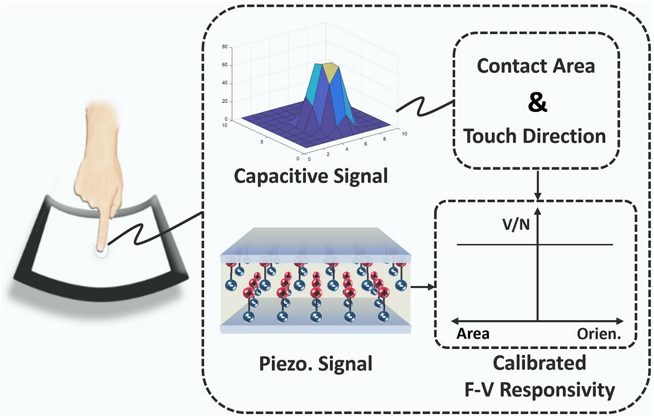

FIGURE 1. Conceptual description of utilizing touch-induced capacitive information to maintain the force-voltage responsivity for piezoelectric touch panel.

explains the relationship between capacitive and force information and proposed touch area and orientation interpretation algorithm. Section IV describes the testbed. Experimental results and discussion are provided in Section V. Finally, conclusions are drawn in Section VI.

II. CHALLENGES TOWARDS HIGH DETECTION ACCURACY

A. INSTABLE FORCE-VOLTAGE RESPONSIVITY ISSUE IN PIEZOELECTRIC FORCE TOUCH PANEL

The piezoelectric force touch panels can detect force-induced stress in the z direction. When a force touch is applied, the polarization of the piezoelectric material changes, generating electric signals. Assuming a perpendicular force event occurs, the relationship between the applied force and the generated charges in scalar expression is:

$$P_i = d_{ij}\sigma_{ij} \tag{1}$$

where $\sigma = F/A \cdot P$ is the induced polarization, d and σ represent the piezoelectric coefficient and force applied stress. F and A denote applied force and the contact area. Hence, with different contact areas, the same force amplitude gives rise to different polarization shifts [10]. Furthermore, if the force direction is not perpendicular, which is more likely to happen in practice, the force component in the z direction could be unpredictable without the information of touch orientation [10], resulting in an inaccurate force interpretation.

B. FINGER TOUCH-INDUCED CAPACITIVE INFORMATION

The characteristics of a finger touch-induced capacitance change are widely used for the determination of touch location [11], sliding direction and avoiding registration of fake touches, e.g., cheek touch [13]. In [14], finger movement-induced capacitance change is used for yaw control, such as twist, pan, zoom and, 3D manipulation. However, previous work mainly reports on the use of the capacitive information for touch action recognition (e.g., touch or swipe, the precise detection of contact area and touch angle, especially during force touch events, are omitted Hence, in the next section, we investigate the force touch associated finger characteristic.

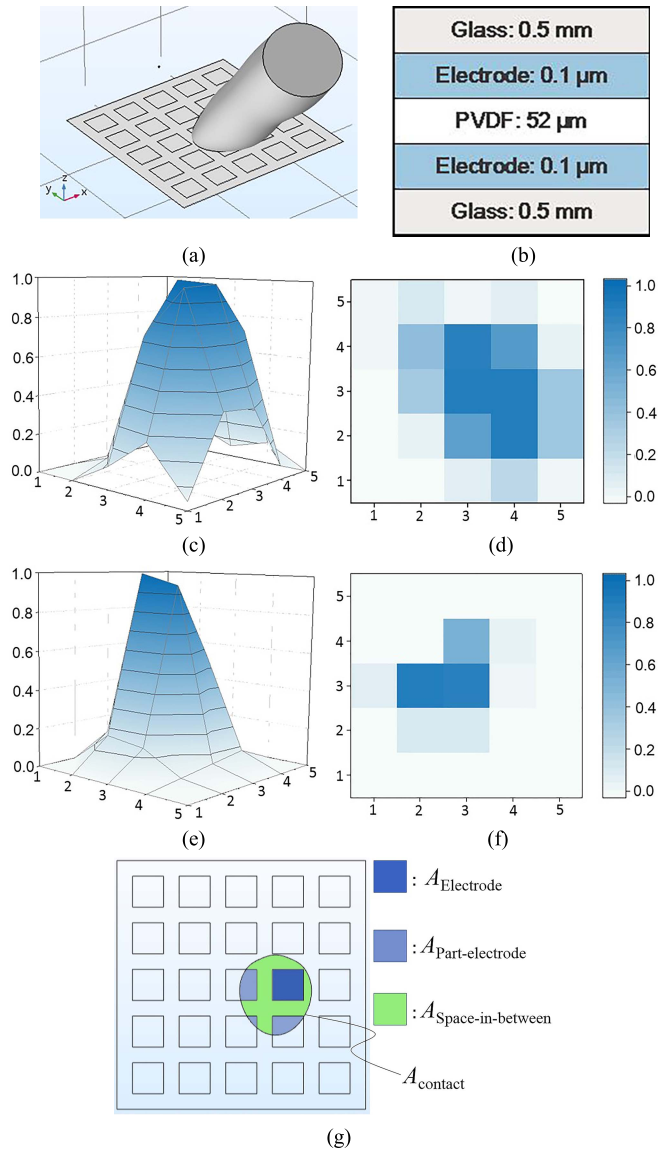

FIGURE 2. (a) Touch panel with finger model in COMSOL simulation environment. (b) Structure of the touch panel. (c) and (d) Are the projection-view and intensity map of the simulated capacitance distribution of a finger touch at the 15° touch angle. (e) and (f) Are the projection-view and intensity map of simulated capacitance distribution of a finger touch at the 90° touch angle. (g) Is the contact area and its components.

III. STUDY ON FORCE TOUCH RELATED CAPACITIVE INFORMATION

A. SIMULATION ENVIRONMENT AND SETUP

To accurately model the finger-induced capacitance change, a capacitive touch panel and a human index finger are simulated, as shown in Fig. 2a. In our previous studies, COMSOL software has been proved to be a validate simulation environment to probe the characteristics of piezoelectric touch panels, and fully clamped boundary conditions were applied to the touch panel models. In this study, we adopt the same boundary condition as used in [1]. However, in the current model, we don't simulate four supporting frames as created in [1], alternatively, four rectangular planes were attached to the bottom of the touch panel, representing the original four supporting frames. In this way, meshing complexity is reduced without hindering simulation accuracy. In both simulation and experiments, self-capacitance sensing is utilized to measure the capacitance between electrodes to ground. When a finger is approaching to electrodes, original electric field is disturbed, resulting in the capacitance change, which is employed to calculate contact area and touch orientation.

The touch pad consists of three layers: two electrode layers together with their glass substrates, and one dielectric layer (PVDF) in-between. 5×5 ITO electrodes (each takes 5×5 mm^2, spacing at 2 mm) are arranged at the top layer, and a whole ITO electrode (35×35 mm^2) is set as the ground layer. The finger model is from the touchscreen_simulator database [15].

The initial simulated touch position is at the center electrode pad, and then it moves to its adjacent pad along x axis and diagonally with a step of 1 mm, in order to comprehensively study the touch-induced capacitance distributions. Touch angles range from 15^0 to 90^0, with the a step of 15^0. The radius of the finger ranges from 5 to 15 mm.

B. CONTACT AREA ESTIMATION ALGORITHM

Two results are demonstrated in Figs. 2b, c, d, and e, to demonstrate the difference in capacitance distribution induced by various touch angles. It is observed that with the increase in touch angle, the contact area declines, while the slope of the cross-section of the capacitance distribution rises. Hence, by identifying the capacitance distribution, both the contact area and the touch angles can be calculated.

The contact area can be calculated by the equation below:

$$A_{\text{contact}} = NA_{electreode} + \sum_{k=1}^{M} A_{Part\text{-}electrode} + A_{Space\text{-}in\text{-}between} \tag{2}$$

where A_{contact} denotes the contact area, $A_{\text{electrode}}$ the area of a single electrode, and $A_{\text{Part-electrode}}$ the overlapped area between the finger and an electrode. Note that $A_{\text{Part-electrode}}$ is smaller than $A_{\text{electrode}}$, since only a part of the electrode is contacted. $A_{\text{Space-in-between}}$ represents the area between the contacted electrodes. M and N are positive integers representing numbers of $A_{\text{Part-electrode}}$ and $A_{\text{electrode}}$. To obtain A_{contact}, the key is to calculate M, N and $A_{\text{Space-in-between}}$. An example of contact area is shown in Fig. 2f.

To determine $A_{\text{Part-electrode}}$, the relationship between capacitance value and contact area is investigated here. In Fig. 2, the capacitance values are normalized. Therefore, the capacitance value of "1" indicates a full contact. A capacitance value smaller than unity can be used to obtain the contact area through (2):

$$A_{\text{Part-electrode}} = C_{\text{norm}} \times A_{\text{electrode}} \tag{3}$$

It can be assumed that when C_{norm} is smaller than 0.1, the capacitance change is deemed not-induced by the finger contact. However, following limitations are suffered: first, when the finger is just above the sensor without physical contact, the induced capacitance change may be taken into consideration for area calculation, resulting in a larger contact area value. Although we set a threshold to remove this, inaccuracy interpretation still exists. Second, the status of the finger may bring inaccuracy. For example, when a glove touch is applied, the touch induced capacitance change would be smaller, giving rise to a shrank calculation result.

$A_{\text{Space-in-between}}$ consists of five components: (a) the space between two fully contacted electrodes; (b) the space between a fully contacted electrode and a partly contacted electrode; (c) the space between two partly electrodes; (d) the space between a fully contacted electrode and a non-contacted electrode; (e) the space between a partly contacted electrode and a non-contacted electrode. For the cases (a) and (b), a full space area is occupied. As to the case (c) to (e), a scaling factor α is used to apply to the space area, hence:

$$\alpha = (C_{\text{Electrode1}} + C_{\text{Electrode2}})/2C_{\text{Full}} \tag{4}$$

where $C_{\text{Electrode1}}$ and $C_{\text{Electrode2}}$ are the capacitance values at the two partly contacted electrodes, while C_{Full} indicates the capacitance value of a fully contacted electrode. In some scenarios, a space area is calculated twice, since case (b) and (c) occur for the same area; therefore, only the higher value is kept by the algorithm, whereas the lower is discarded. The pseudocode of the algorithm is shown in Fig. 3.

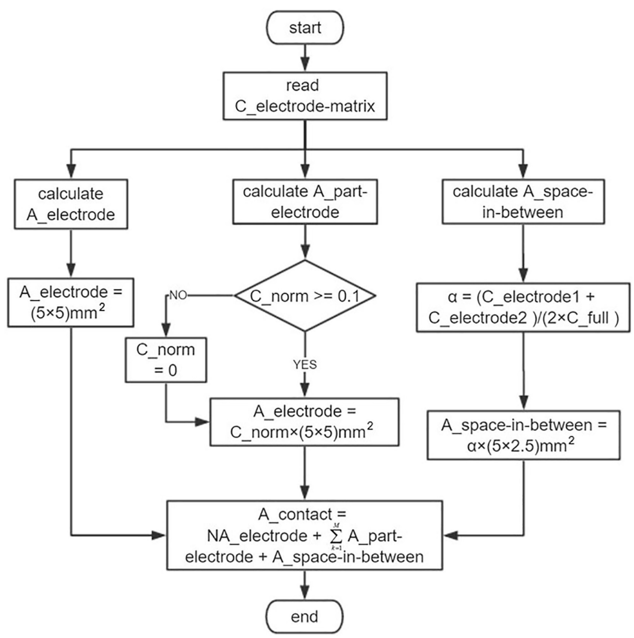

FIGURE 3. **Flowchart of the algorithm for calculating the touch area.**

The proposed area estimation algorithm can offer an overall accuracy of 94.2%. After obtaining the calculated contact area, the force amplitude can be calculated by Hooke's Law.

C. TOUCH ANGLE ESTIMATION ALGORITHM

The interpretation of touch angle relies on the recognition of the trend of touch-induced capacitance change. Current literature [16]–[18] makes use of elaborate algorithms which consume considerable processing resources. In this work both capacitive and force signal are required to be calculated, and a less computational complex algorithm is proposed by using the distance between the capacitance change at the touch position and the minimum touch-induced capacitance.

The touch position can be determined by:

$$I(x, y) = I_b + I_p \exp\left(-\frac{(x-u)^2 - (y-u)^2}{2\sigma^2}\right) \quad (5)$$

where $I(x, y)$ is the capacitance intensity at a given location of the touch panel, I_b denotes intensity of the background offset, I_p represents the peak intensity, and (u, v) the touch location, which is assumed as the center of the finger. As the change of (u, v) is continuous rather than discrete in practice, subpixel algorithms are widely used to interpret the true touch position. In [19], a Gaussian distribution-based algorithm is demonstrated to give the best accuracy for capacitive touch panels, therefore a Gaussian subpixel algorithm is utilized in this work, too, as a subpixel estimator. The Gaussian estimator [19] is:

$$\frac{1}{2}\frac{\ln r_{i-1} - \ln r_{i+1}}{\ln r_{i-1} - 2\ln r_i + \ln r_{i+1}} \quad (6)$$

r_i is the maximum intensity of rows, r_{i-1} and r_{i+1} are the intensities of the adjacent rows. The same algorithm is also applied for columns intensities, to obtain more accurate touch position. Note that the peak intensity is also applied by the Gaussian subpixel algorithm.

As mentioned above, the distance is also determined by the position of minimum touch-induced capacitance change, which is constrained by the system's sensitivity. Since the performance of sensitivity varies for different systems, a signal-to-noise ratio (SNR) of 20dB is assumed, which is an easy-to-achieve value for most capacitive touch panel systems [20]. Hence, the minimum touch-induced capacitance is one order smaller than the peak intensity. With the use of the simulation results, the relationship between distance and touch orientation is created as shown in Fig. 4.

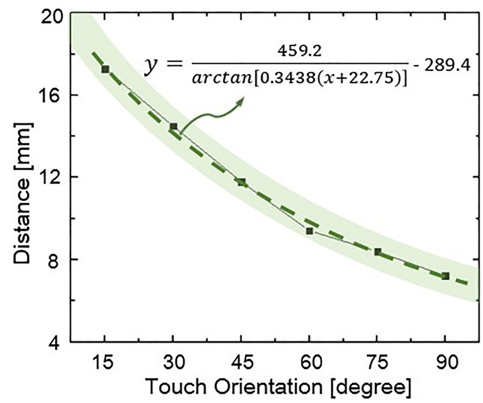

FIGURE 4. Relationship between touch orientation and distance.

IV. TESTBED DESCRIPTION AND ARTIFICIAL FINGER FABRICATION

A. TOUCH PANEL FABRICATION

A piezoelectric touch panel is assembled for validating the proposed methods. ITO/PVDF/ITO based structure is utilized for constructing the touch panel. The top layer ITO is patterned to be 5×5 eventually distributed squares (5×5 mm^2, spacing at 2 mm), acting as sensing electrodes. The bottom ITO operates as the ground layer. The photograph of the touch panel is shown in Fig. 5a.

B. BIONIC FINGER FABRICATION

To accurately apply the touch event in terms of force amplitude and touch angle, a bionic finger is fabricated. Gelatin, whose physical and electrical property is close to human skin [21], is selected for the artificial finger fabrication. The fabrication process is as follows. First, the gelatin powder (cowhide Inc.) and water are thoroughly mixed, with the help of magnetic stirrer, in a ratio of 1 to 4 after heating and stirring. When gelatin is completely dissolved, the solution is poured into a finger mold, in which a copper stick is settled to mimic the finger bone. After 24 hours at room temperature, the artificial finger is obtained, as shown in Fig. 5b. The electric conductivity and Young's modulus of the artificial finger are 0.2S/m (10kHz) and 40kPa, respectively, and they are close to those of a human finger [22], [23].

The end of the copper stick is attached to a force meter [24], hence the applied force amplitude can be measured.

C. SYSTEM INTEGRATION

The technique for concurrently reading out the capacitive and force information is borrowed from our previous research [1]. The system block diagram and photograph of the readout circuit are shown in Fig. 5c. Experiments are performed on a flat substrate, which indicates a fully compressed condition. The practical operating conditions of a touch panel in an interactive display is closer to a simple supported case. Nevertheless, the target of this study is to estimate the real user applied force amplitude, via finding the relationship between touch-induced force signal and capacitive signal, hence only the simplest mechanical condition is used to remove any interference introduced by inaccurate mechanical condition setup.

V. RESULTS AND DISCUSSION

The force response is normally expressed as coulombs per newton (C/N), as charges are induced by applied force events. The response is also widely expressed as voltage per newton in some studies, as voltage amplitudes are the inputs for analogue-to-digital converters. The transfer function for

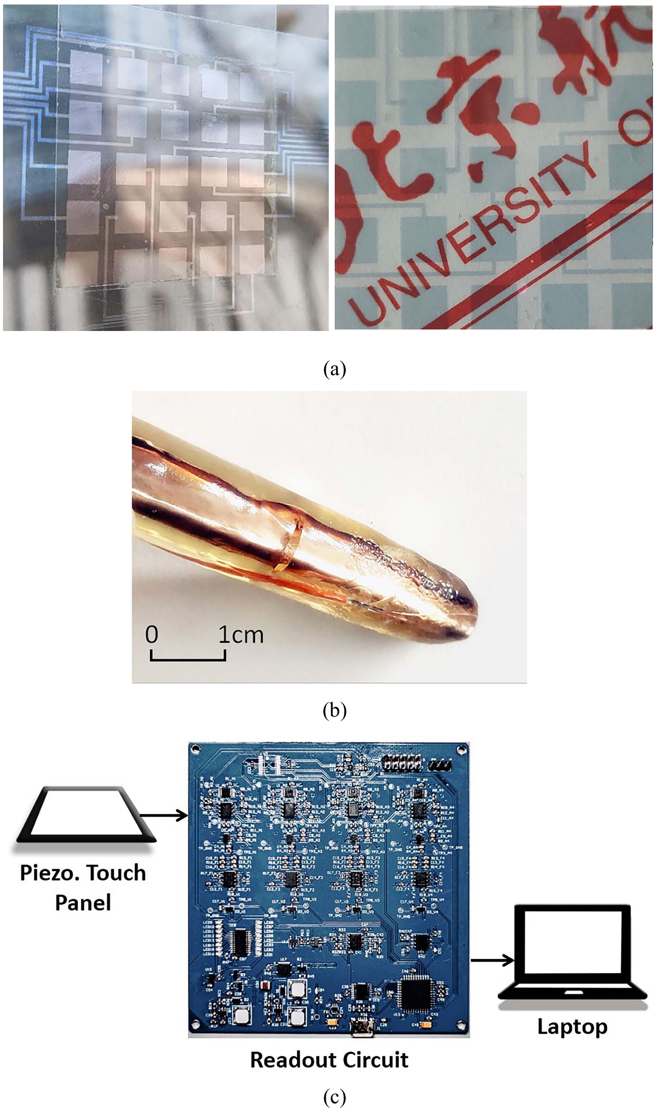

FIGURE 5. **(a) Fabricated touch panel. (b) Gelatin based artificial finger. (c) Blockdiagram of touch panel system and readout circuit.**

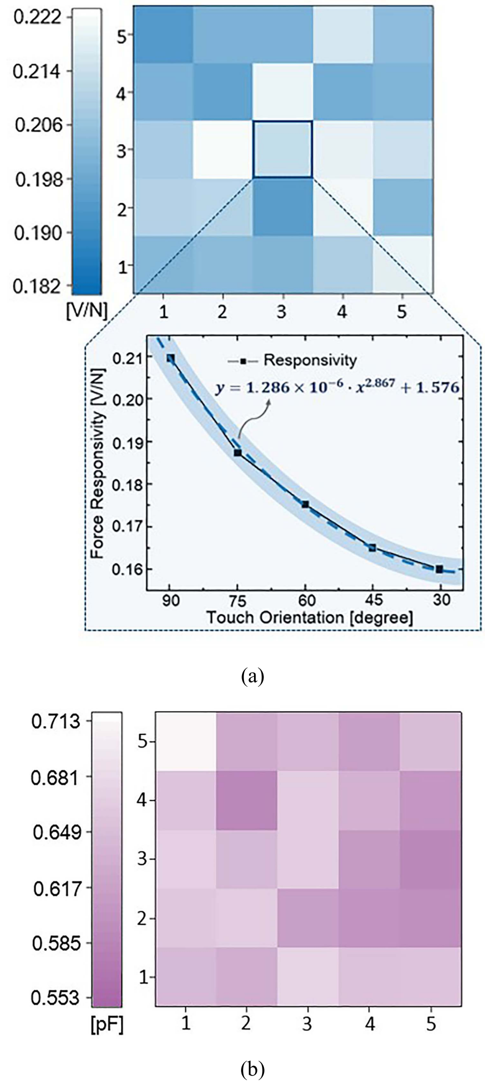

FIGURE 6. **(a) Force touch responsivity of the fabricated touch panel. (b) The capacitance offsets at each electrode are shown.**

voltage based responsivity is expressed as below [3]:

$$V = \frac{Q}{C} = \frac{d_{33} F T}{\varepsilon_o \varepsilon_r A} \tag{7}$$

where t represents the thickness of the piezoelectric film, ε_o and ε_r indicate the vacuum permittivity and the relative permittivity of the piezoelectric layer, respectively.

A. TOUCH PANEL PERFORMANCE

In the proposed method, the non-uniform force-voltage responsivity is calibrated by the capacitive information; hence, the system performance in terms of force and capacitive sensing are examined. For the former, the piezoelectric coefficients (d_{33}) at each electrode position are tested and the corresponding results are shown in Fig. 6a. It is observed that the measured d_{33} values present a good uniformity, and a mean value at 199 mV/N is obtained. The performance of force-voltage responsivity at different touch orientations at the center location is also illustrated in Fig. 6a, demonstrating a negative correlation between the touch orientation and the force-induced voltage value, aligning with our expectation. Note that the correlation can be modeled as shown in the figure, however the model accuracy might shift for different touch object. The relationship between contact area and force amplitude is align with the Hooke's law.

As to the latter, the capacitance offsets are examined, due to their importance for capacitive touch registration [20]. Experiments are carried out by a network analyzer, and results are plotted in Fig. 6b.

B. FORCE TOUCH DETECTION WITH THE CALIBRATION ALGORITHM

In this subsection, an example of how the force amplitude is calibrated is provided, and then the overall performance of the algorithm is presented.

Traditionally, the force induced voltage signal is used to interpret the force level by using the equation [3]:

$$Q = d_{33}F \tag{8}$$

where Q is the collected charges, F the applied normal force. With the orientation information and the relationship between touch orientation and force responsivity, we learn that the calibrated $d'_{33} = f(d_{33})$, where f is expressed in Fig. 6 a. In terms of the contact area, we noticed that some force components are applied at electrode free zones as stated previously, hence, no charges are collected, lowering detection accuracy. In our algorithm, an assumption is made that the force at the contact area is uniformly distributed. Hence, we use the stress value at one fully contact area to estimate the total stress by:

$$Q' = Q\left(\frac{A_{Contact}}{A_{Electrode}}\right) \tag{9}$$

Hence, the calibrated force is:

$$F' = \frac{Q'}{d'_{33}} \tag{10}$$

A strong force touch event from an arbitrary orientation is applied at the center of the touch panel. The force-induced voltage and capacitance distributions are illustrated in Fig. 7. Based on previous force interpretation methods found in the literature [1], [25], a force value of approximately 3.4 N is obtained. However, the force value reading by the force meter is 5.2 N, which is much higher than the interpreted value. Alternatively, based on the algorithm proposed in this paper, a contact area of 1.7 cm^2 and a touch orientation of 34^0 are yielded via processing the capacitive information. In fact, the calibrated force value is 4.9 N, approaching to the force meter reading by 29%, demonstrating the suitability and the advanced performance of the proposed method.

Overall performance is provided in Fig. 8. The artificial finger performs touch events from 5 different angles (30 times for each angle, and from 30^0 to 90^0 with a step 15^0). Among them, the 90^0 experiment gives the best result (97%), and the detection accuracy slightly drops with the decrease of touch orientation. This is mainly due to the characteristics of the fabricated artificial finger which does not perfectly match the nature of the human finger, as used in the COMSOL simulation. Specifically, the fact of less conductive issue of the artificial finger results in the misinterpretation of the touch orientation and contact area. With human finger touch events, better results should be expected. Furthermore, in our touch orientation algorithm, distance is the only parameter utilized to interpret touch angle. Nevertheless, this method doesn't always provide high detection accuracy, as other characteristics of fingers, such as finger size, shape and rigidity, can influence calculation accuracy. Hence, in our experimental results, the highest accuracy appears at 90 degree, and the results is getting worse with the decrease of touch orientation. In future research, the estimation of touch orientation requires to put a comprehensive consideration of characteristics of fingers.

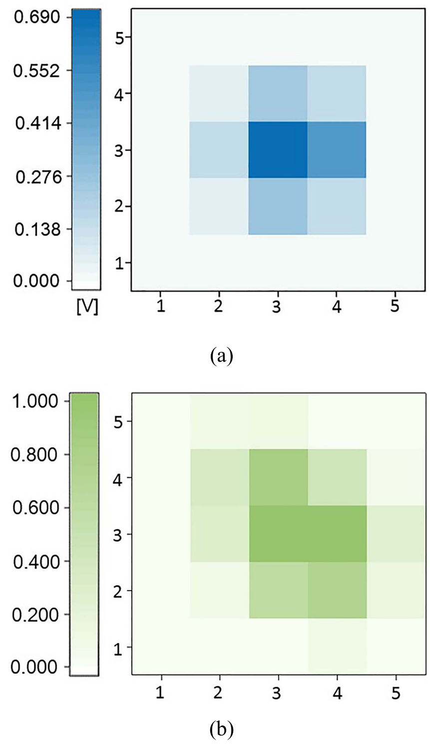

FIGURE 7. **(a) Voltage and (b) Normallized capacitance distributions of the applied force touch event.**

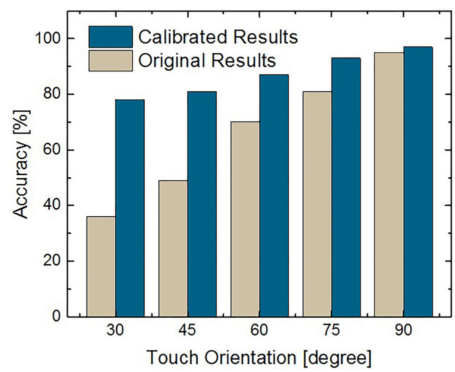

FIGURE 8. **Detection accuracy of the proposed algorithm vs different touch orientations.**

C. TIME AND POWER BUDGET ESTIMATION

Although the presented technique boosts the force detection accuracy of piezoelectric based force touch panels, the computational costs in terms of time and power consumption are important when considering implementing this technique to commercial touch panel products.

Current touch panels scan a full screen at 60 Hz, by employing 16×9 electrode bars, denoting that the time interval for running the algorithm is smaller than 16.7 ms for the 144 pixels. The algorithm's time complexity for this work is $O(3N)$, since capacitive information is used twice, and force information is calculated once. Considering a 1 GHz processor used for the touch panel system, the time cost is 0.432 µs, which is far shorter than the scanning interval.

The estimation of power budget is based on the power efficiency of mainstream commercial processors, whose capabilities are over 20 MIPS/mW [26], [27]. Hence, the estimated power budget is 21.6 nW, which is negligible compared to the power consumption of commonly used touch panel controllers.

VI. CONCLUSION

In this article, we present a calibration method for improving the stability of force-voltage responsivity in piezoelectric based touch panel for interactive displays. Here, user-induced instable force responsivity is addressed by smartly using touch generated capacitive information. The work in this paper not only showcases a technique for stabilizing force responsivity, but also demonstrate the use of multidimensional information to accurately reconstruct the original stimulus.

ACKNOWLEDGMENT

The authors acknowledge Cambridge Touch Technologies (Cambridge, U.K.) for their generous provision of the touch panel stack-up and readout circuit architectures, and the funding from Beihang University.

REFERENCES

[1] S. Gao, V. Arcos, and A. Nathan, "Piezoelectric vs. capacitive based force sensing in capacitive touch panels," *IEEE Access*, vol. 4, pp. 3769–3774, 2016.
[2] S. Yue and W. A. Moussa, "A piezoresistive tactile sensor array for touchscreen panels," *IEEE Sensors J.*, vol. 18, no. 4, pp. 1685–1693, Feb. 2018.
[3] S. Gao, X. Wu, H. Ma, J. Robertson, and A. Nathan, "Ultrathin multifunctional graphene-PVDF layers for multidimensional touch interactivity for flexible displays," *ACS Appl. Mater. Interfaces*, vol. 9, no. 22, pp. 18410–18416, 2017.
[4] S. Gao, J. Duan, V. Kitsos, D. R. Selviah, and A. Nathan, "User-oriented piezoelectric force sensing and artificial neural networks in interactive displays," *IEEE J. Electron Devices Soc.*, vol. 6, pp. 766–773, Jun. 2018. [Online]. Available: https://ieeexplore.ieee.org/document/8391712
[5] S. Gao, Y. Dai, V. Kitsos, B. Wan, and X. Qu, "High three-dimensional detection accuracy in piezoelectric-based touch panel in interactive displays by optimized artificial neural networks," *IEEE Sensors J.*, vol. 19, no. 4, p. 753, Feb. 2019.
[6] M. Ando, H. Kawamura, H. Kitada, Y. Sekimoto, T. Inoue, and Y. Tajitsu, "Pressure-sensitive touch panel based on piezoelectric poly (L-lactic acid) film," *Jpn. J. Appl. Phys.*, vol. 52, no. 9S1, Sep. 2013, Art. no. 09KD17.
[7] M.-W. Kim *et al.*, "Thermal-variation insensitive force-touch sensing system using transparent piezoelectric thin-film," *IEEE Sensors J.*, vol. 18, no. 14, pp. 5863–5875, Jul. 2018.
[8] M. Kang *et al.*, "Fully flexible and transparent piezoelectric touch sensors based on ZnO nanowires and $BaTiO_3$-added SiO_2 capping layers," *Physica Status Solidi (A)*, vol. 212, no. 9, pp. 2005–2011, Sep. 2015.
[9] A. Nathan, J. C. S. Lai, S. Cha, and C. Church, "Pressure sensing display device," U.S. Patent 20 140 008 203 A1, Jan. 9, 2014.
[10] S. Gao and L. Wu, "Why piezoelectric based force sensing is not successful in interactive displays," *IEEE Trans. Consum. Electron. Mag.*, to be published.
[11] Z. Baharav and R. Kakarala, "Capacitive touch sensing: Signal and image processing algorithms," in *Proc. Comput. Imag. IX*, vol. 7873. San Francisco, CA, USA, 2011, Art. no. 78730H. [Online]. Available: https://doi.org/10.1117/12.876714
[12] M. G. A. Mohamed *et al.*, "Efficient algorithm for accurate touch detection of large touch screen panels," in *Proc. 18th IEEE Int. Symp. Consum. Electron. (ISCE)*, 2014, pp. 1–2.
[13] G. Walker, "A review of technologies for sensing contact location on the surface of a display," *J. Soc. Inf. Display*, vol. 20, no. 8, pp. 413–440, Aug. 2012.
[14] R. Xiao, J. Schwarz, and C. Harrison, "Estimating 3D finger angle on commodity touchscreens," in *Proc. Int. Conf. Interact. Tabletops Surfaces*, 2015, pp. 47–50.
[15] COMSOL. *Application.Touchscreen_Simulator*. Accessed: Apr. 25, 2019. [Online]. Available: http://cn.comsol.com/model/touchscreen-simulator-30841
[16] M. Badaye, J. R. Peterson, and D. P. Funston, "Touch orientation calculation," U.S. Patent 9 304 622, Apr. 2016.
[17] S. Rogers, J. Williamson, C. Stewart, and R. Murray-Smith, "AnglePose: Robust, precise capacitive touch tracking via 3D orientation estimation," in *Proc. ACM SIGCHI Conf. Human Factors Comput. Syst. (CHI)*, Vancouver, BC, Canada, 2011, pp. 2575–2584.
[18] F. Wang, X. Cao, X. Ren, and P. Irani, "Detecting and leveraging finger orientation for interaction with direct-touch surfaces," in *Proc. 22nd Annu. ACM Symp. User Interface Softw. Technol.*, Victoria, BC, Canada, 2019, pp. 23–32.
[19] A. Braun, R. Wichert, A. Kuijper, and D. W. Fellner, "Capacitive proximity sensing in smart environments," *J. Ambient Intell. Smart Environ.*, vol. 7, no. 4, pp. 483–510, 2015.
[20] S. Gao, J. Lai, C. Micou, and A. Nathan, "Reduction of common mode noise and global multivalued offset in touch screen systems by correlated double sampling," *J. Display Technol.*, vol. 12, no. 6, pp. 639–645, Jun. 2016.
[21] S. B. Lee, Y. H. Kim, M. S. Chong, S. H. Hong, and Y. M. Lee, "Study of gelatin-containing artificial skin V: Fabrication of gelatin scaffolds using a salt-leaching method," *Biomaterials*, vol. 26, no. 14, pp. 1961–1968, May 2005.
[22] P. A. Hasgall *et al.* (May 15, 2018). *IT'IS Database for Thermal and Electromagnetic Parameters of Biological Tissues, Version 4.0*. Accessed: Apr. 25, 2019. [Online]. Available: https://itis.swiss/virtual-population/tissue-properties/database/database-summary/
[23] Y. Yu *et al.*, "Multifunctional 'hydrogel skins' on diverse polymers with arbitrary shapes," *Adv. Mater.*, vol. 31, no. 7, pp. 1–9, Feb. 2019.
[24] SUNDOO. *Digital Push & Pull Tester (SH-5)*. Accessed: Apr. 25, 2019. [Online]. Available: http://www.sundoo.com/DetailedProduct.aspx?ID=1002
[25] S. Gao, Y. Shi, Q. Liu, L. Xu, B. Fu, and Z. Yang, "4-dimensional sensing in interactive displays enabled by both capacitive and piezoelectric based touch panel," *IEEE Access*, vol. 7, pp. 33787–33794, 2019.
[26] C. Luo, M. A. Bokar, A. J. Redfern, and J. H. McClellan, "Compressive sensing for sparse touch detection on capacitive touch screens," *IEEE J. Emerg. Sel. Topics Circuits Syst.*, vol. 2, no. 3, pp. 639–648, Sep. 2012.
[27] ARM. *Cortex-A5 Processor Performance*. Accessed: Apr. 25, 2019. [Online]. Available: http://www.arm.com/products/processors/cortex-a/cortex-a5.php

ANBIAO HUANG is currently pursuing the M.Eng. degree with the School of Instrumentation Science and Optoelectronic Engineering, Beihang University, Beijing, China.

SHUO GAO received the Ph.D. degree in electrical engineering from the University of Cambridge, Cambridge, U.K., in 2018. From 2017 to 2018, he was a Research Associate with University College London, London, U.K. He is currently an Associate Professor with Beihang University, Beijing, China. He was an Optical Fiber System Engineer with Ciena Corporation, Ottawa, Canada, from 2012 to 2013; and a Technique Consultant with Cambridge Touch Technologies, Inc., Cambridge, from 2013 to 2017. His area of expertise is human–machine interactive systems. He has published over 20 articles as the first author, including peer-reviewed journals, flagship conferences, awarded U.S., U.K., and CN patents. He was a recipient of the China Scholarship Council Ph.D. Student Fellowship in 2014. He serves on technical committees in various capacities.

YANNING DAI is currently pursuing the undergraduation degree with the School of Instrumentation Science and Optoelectronic Engineering, Beihang University, Beijing, China.

VASILEIOS KITSOS was born in Kavala, Greece, in 1986. He received the Diploma degree in electrical and computer engineering from the Democritus University of Thrace, Greece, in 2010, and the M.S. degree in biomedical engineering from Imperial College London, U.K., in 2011. He is currently pursuing the Ph.D. degree in electronic and electrical engineering with University College London, U.K.

In 2012, he joined Maltron International Ltd., where he participated in the development of an electrical impedance tomography system to use on neonates. His doctoral research focuses on the development of low-power, miniaturized flow sensors for respiratory monitoring. He holds a fully funded scholarship from the Engineering and Physical Sciences Research Council. His research interests also include energy-efficient temperature and humidity sensors for biomedical applications.

WENBIN TIAN received the B.Eng. degree in electrical engineering from Sichuan University, China, in 2011, and the M.Sc. and Ph.D. degrees in microwave and communication engineering from the University of Manchester, U.K., in 2013 and 2018, respectively. He is currently a Post-Doctoral Research Fellow with Beihang University, Beijing, China. His current research interests include electrical capacitance tomography, sensor design, and image processing.

LIJUN XU (M'04–SM'14) received the B.Sc., M.Eng., and Ph.D. degrees in electrical engineering and instrumentation from Tianjin University, Tianjin, China, in 1990, 1993, and 1996, respectively.

From 1997 to 2001, he was an Associate Professor with Tianjin University. From January 2002 to April 2006, he was a Research Fellow with the University of Greenwich and University of Kent, and a Higher Scientific Officer with the Institute of Cancer Research, U.K. He is currently a Professor and the Dean of the School of Instrumentation Science and Opto-Electronic Engineering, Beihang University, Beijing, China. He has authored or coauthored over 260 publications. His current research interests include tomographic imaging, scanning imaging, and dynamic process monitoring.

Dr. Xu was a recipient of the National Science Fund for Distinguished Young Scholars in 2012, the Ministry of Education Technology Invention Award (First Class) in 2012, and the China Instrument Society Science and Technology Award (First class) in 2014. He was elected as a Chang-Jiang Scholars Program Professor and a National High-Level Personnel of Special Support Program by the Ministry of Education, Ministry of Organisation, China, in 2014 and 2016, respectively.